BULLETIN OF THE EARTHQUAKE
RESEARCH INSTITUTE
Vol. 45 (1967), pp. 785-798

41. *Geomagnetic Variation Associated with Stress Change Within a Semi-infinite Elastic Earth Caused by a Cylindrical Force Source.*

By Takesi YUKUTAKE and Hiroko TACHINAKA,

Earthquake Research Institute.

(Read April 25, 1967.—Received June 30, 1967.)

Summary

Geomagnetic variations are studied due to the effect of stress on magnetization of rocks when a hydrostatic pressure is applied from inside to the cylindrical surface embedded in the earth. If the earth is assumed to be composed of a homogeneous rock with an intensity of magnetization 3×10^{-3} emu/cc, the maximum change of approximately 2γ in total intensity is expected for the cylindrical source of 5 km radius being placed at a depth of 14.5 km and subjected to an internal pressure of 100 bar. For the cylinder of 10.5 km depth, the variation amounts to 3γ.

1. Introduction

It has long been a matter of dispute whether any change in the geomagnetic field can be observed in association with an earthquake. It is attempted in this paper to estimate a possible variation in the field caused by the stress effect on magnetization of rocks.

The stress effect on the magnetic susceptibility was experimentally studied by Kalashnikov and Kapitsa[1], Grabovsky and Parkhomenko[2], Domen[3] and Nagata and Kinoshita[4]. It was also investigated theoretically by Stacey[5] and Nagata[6]. All these studies can be summarized by stating that the magnetization in the direction of compression is decreased, whereas the magnetization perpendicular to the applied com-

1) A. G. KALASHNIKOV and S. P. KAPITSA, *Doklady Akad. Nauk SSSR*, **86** (3), (1952) 521.
2) M. A. GRABOVSKY and E. I. PARKHOMENKO, *Izvest. Akad. Nauk SSSR, Ser. Geofiz.*, **5** (1953), 405.
3) H. DOMEN, *Jour. Geomag. Geoelect.*, **13** (1962), 66.
4) T. NAGATA and H. KINOSHITA, *Jour. Geomag. Geoelect.*, **17** (1965), 121.
5) F. D. STACEY, *Phil. Mag.*, **7** (1962), 551.
6) T. NAGATA, *Jour. Geomag. Geoelect.*, **18** (1966), 73 and 411.

pression is slightly increased.

On the basis of the above experimental results, Stacey attempted to estimate possible variations in the geomagnetic field at the times of earthquakes and volcanic eruptions. Assuming a specific distribution of stress due to a fault, he obtained a maximum variation in the magnetic field of 40γ for the earth model composed of igneous rocks having the remanent magnetization of 10^{-2} emu when a peak stress in the fault is assumed as 100 kg/cm^2, and 4γ for the earth model of remanent magnetization of 10^{-3} emu[7]. He also calculated magnetic changes associated with stress fields when a spherical magma chamber beneath a volcano is under a critical condition for tensile and shear failure[8], obtaining a local maximum effect of 7γ. In his calculation of stress distribution, however, he ignored boundary conditions for stresses at the ground surface. This simplification does not seem relevant to the present problem. The magnetic change to be observed at the ground surface is greatly affected by changes in the magnetization of shallow origin.

In relation to the study of the earthquake mechanism, a number of theoretical works have been conducted on simple models to obtain stress and strain distributions. When a sphere is embedded in a semi-infinite elastic medium, and various types of stress distribution are given on its surface, stress and strain distributions at the ground surface were calculated by Soeda[9] and Yamakawa[10]. Recently, Rikitake developed a theory for the cylindrical source model, in which a hydrostatic pressure is applied from inside[11]. In these studies, boundary conditions for stresses and strains at the ground surface are taken into consideration, whereas those at the spherical or the cylindrical surface are ignored.

In this paper, magnetic variation is calculated on the basis of Rikitake's work, which seems more relevant to calculate the magnetic variation at the surface than does Stacey's model.

In section 2, Rikitake's theory is outlined and the distributions of stresses and strains within the earth are computed. Changes in the remanent magnetization associated with the stress changes are calculated in section 3 and numerically integrated in such a way as to give the magnetic variation at the ground surface.

---

7) F. D. STACEY, *Pure Appl. Geophys.*, **58** (1964), 5.
8) F. D. STACEY, K. G. BARR and G. R. ROBSON, *Pure Appl. Geophys.*, **62** (1965), 96.
9) K. SOEDA, *Quart. Jour. Seism.*, **11** (1940), 256; **13** (1944), 263.
10) N. YAMAKAWA, *Zisin*, **8** (1955), 84.
11) T. RIKITAKE, Unpublished note.

2. Stresses and strains produced by a cylindrical source

Rikitake studied a stress-strain problem when a cylinder is embedded within a half space and a hydrostatic pressure is applied from inside the cylinder.[11]

Firstly, stresses and displacements when the cylinder of radius a is placed in an unbounded space and subjected to a hydrostatic pressure $(-p_0)$ from inside are calculated. When the Cartesian coordinates (x, z) and the polar coordinates (r, θ) are taken as in Fig. 1, displacements and stresses outside the cylinder are obtained as follows:

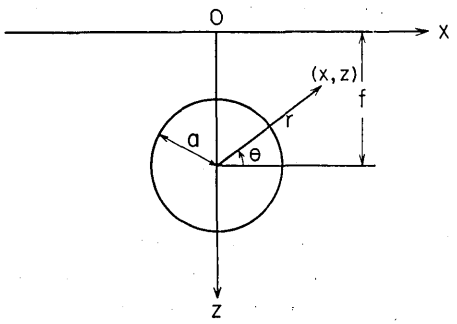

Fig. 1. Coordinate system.

$$\left.\begin{aligned} u_x &= \frac{a^2 p_0}{2\mu}\,\frac{x}{x^2+(z-f)^2} \\ u_z &= \frac{a^2 p_0}{2\mu}\,\frac{z-f}{x^2+(z-f)^2} \end{aligned}\right\} \tag{1}$$

$$\left.\begin{aligned} \tau_{rr} &= -p_0 a^2 \frac{1}{x^2+(z-f)^2} \\ \tau_{\theta\theta} &= -p_0 a^2 \frac{1}{x^2+(z-f)^2} \end{aligned}\right\} \tag{2}$$

where u_x, u_z are the x and z components of displacement and τ_{rr}, $\tau_{\theta\theta}$ are the rr and $\theta\theta$ components of stress tensor. μ designates rigidity, f the depth to the center of the cylinder.

At the ground surface $z=0$ the normal stress τ_{zz} and tangential shear stress τ_{xz} are required to vanish. Let us take the solutions produced by a cylindrical source with the same intensity $-p_0$ at a mirror point $(z=-f)$, the displacements being given as

$$\left.\begin{aligned} u_x &= \frac{a^2 p_0}{2\mu}\,\frac{x}{x^2+(z+f)^2}\,, \\ u_z &= \frac{a^2 p_0}{2\mu}\,\frac{z+f}{x^2+(z+f)^2}\,, \end{aligned}\right\} \tag{3}$$

On superposing them on the above solutions (1) and (2), τ_{xz} vanishes at the ground surface. However, τ_{zz} remains finite:

$$\tau_{zz}=2a^2p_0\frac{x^2-f^2}{(x^2+f^2)^2} \qquad \text{at } z=0\,. \tag{4}$$

In order to cancel the normal stress at the surface, we may add the following displacements to those given in (1) and (3). Such a procedure does not disturb the boundary condition for τ_{zz}.

$$\left.\begin{aligned} u_x'&=a^2p_0\left[\frac{1}{\lambda+\mu}\,\frac{x}{x^2+(z+f)^2}-\frac{1}{\mu}\,\frac{2xz(z+f)}{\{x^2+(z+f)^2\}^2}\right],\\ u_z'&=-a^2p_0\left[\frac{\lambda+2\mu}{\mu(\lambda+\mu)}\,\frac{z+f}{x^2+(z+f)^2}-\frac{1}{\mu}\,\frac{z\{x^2-(z+f)^2\}}{\{x^2+(z+f)^2\}^2}\right], \end{aligned}\right\} \tag{5}$$

where λ is a Lame's constant.

For simplicity, here we assume $\lambda=\mu$. Then the solutions which satisfy the boundary conditions are given as follows,

$$\left.\begin{aligned} u_x&=u_{x0}+u_x'\,,\\ u_z&=u_{z0}+u_z'\,,\\ u_{x0}&=\frac{a^2p_0}{2\mu}\,x\left[\frac{1}{x^2+(z-f)^2}+\frac{1}{x^2+(z+f)^2}\right],\\ u_{z0}&=\frac{a^2p_0}{2\mu}\left[\frac{z-f}{x^2+(z-f)^2}+\frac{z+f}{x^2+(z+f)^2}\right],\\ u_x'&=-\frac{a^2p_0}{2\mu}\,\frac{x}{\{x^2+(z+f)^2\}^2}[3z^2+2fz-f^2-x^2]\,,\\ u_z'&=-\frac{a^2p_0}{2\mu}\,\frac{1}{\{x^2+(z+f)^2\}^2}[5z^3+13fz^2+11f^2z+3f^3+3fx^2+x^2z]\,. \end{aligned}\right\} \tag{6}$$

Principal stresses (τ_1, τ_2) outside the cylinder and their directions (l_1, n_1), (l_2, n_2) are easily obtained as

$$\left.\begin{aligned} \tau_i&=\frac{\tau_{xx}+\tau_{zz}\pm\sqrt{(\tau_{xx}-\tau_{zz})^2+\tau_{xz}^2}}{2}\,,\\ \nu_i&=\frac{2(\tau_i-\tau_{xx})}{\tau_{xz}}\,, \end{aligned}\right\} \tag{7}$$

where $\nu_i=\dfrac{n_i}{l_i}=\tan\varphi$ $(i=1, 2)$.

For a few cases, the strain and stress distributions were calculated at an interval of 1 km in the x-direction and at intervals of 1 m for $0\leqq z\leqq 10$ m, 10 m for $10\text{ m}<z\leqq 100$ m, 100 m for $100\text{ m}<z\leqq 1$ km, 1 km

for 1 km$<z\leqq$20 km. Examples are shown in Fig. 2 and Fig. 3 where p_0 is taken as 10^8 dynes/cm^2 (100 bars) and $\lambda=\mu=10^{12}$ cgs. The cylinder with a radius of 5 km is placed at depths of 14.5 km and 10.5 km. Magnitudes and directions of principal stresses were calculated and are shown in Fig. 4 and Fig. 5, in which tensile stresses are shown by solid lines and compression by broken lines.

Figs. 3 to 5 indicate that the stress τ_{xx}, the nonzero component at the ground surface, changes its sign from positive (tension) to negative (compression) at about 14.5 km distance from the origin when the cylinder is placed at the depth of 14.5 km and at about 10.5 km for the cylinder of 10.5 km depth.

As stated before, the present calculation ignores the boundary condition at the cylindrical surface. Accordingly, the effective stress acting on the cylindrical surface is not a hydrostatic pressure. However, the errors produced by neglecting the boundary condition at the surface

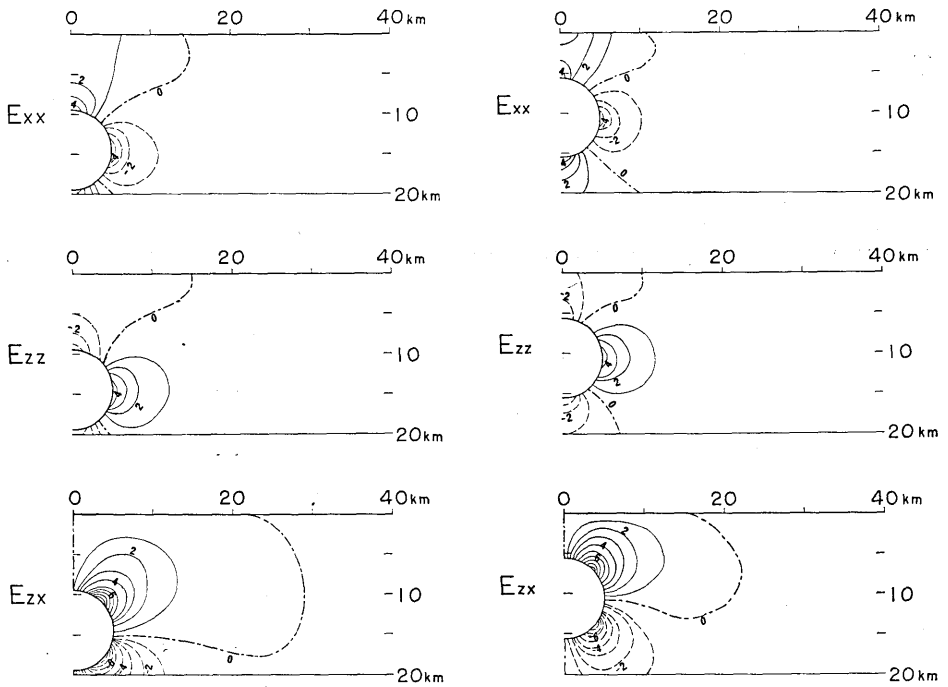

Fig. 2. Distributions of strains when a hydrostatic pressure of 10^8 dynes/cm^2 is applied to the cylindrical surface from inside. From the top to the bottom, e_{xx}, e_{zz} and e_{zx} for the cylinder of 14.5 km depth for (a), and 10.5 km depth for (b). Unit is 10^{-5}.

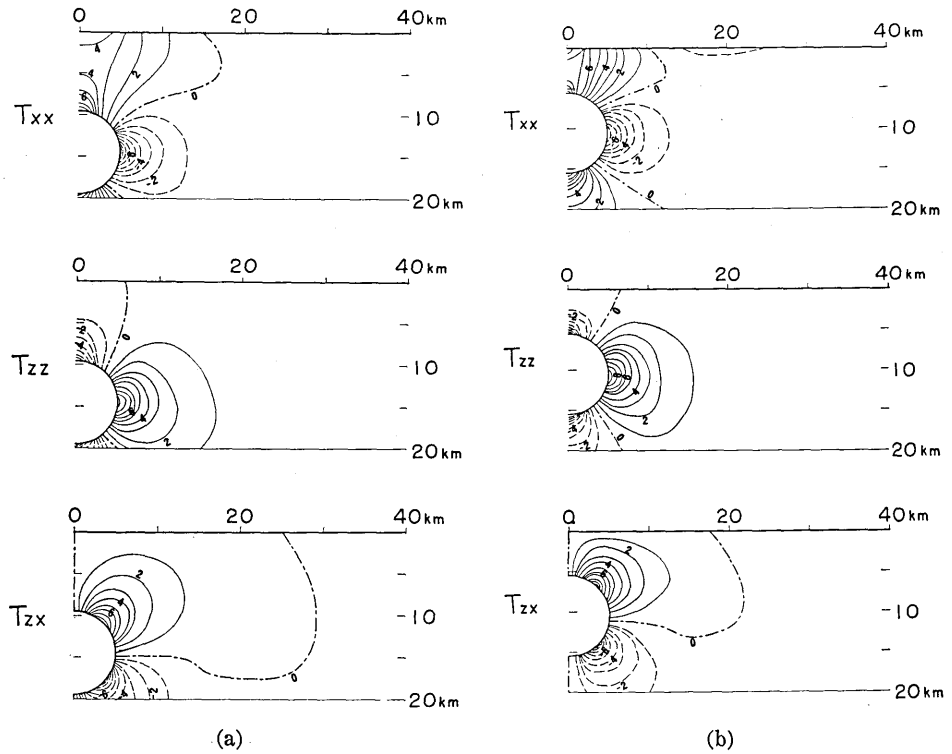

Fig. 3. Distributions of stresses. From the top to the bottom, τ_{xx}, τ_{zz} and τ_{zx} for the cylinder of 14.5 km depth for (a) and 10.5 km depth for (b). Unit is 10^7 dyne/cm^2.

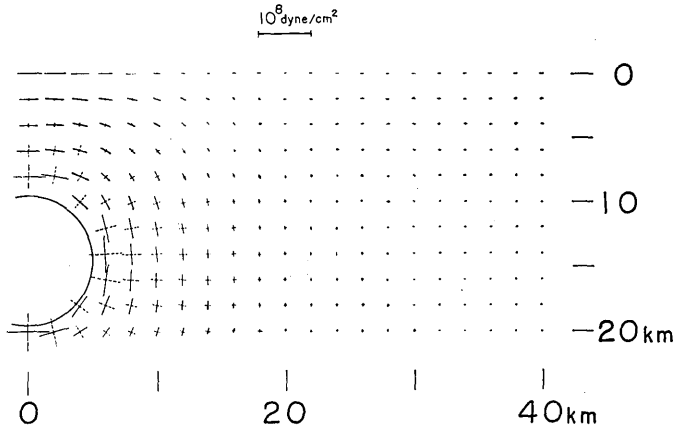

Fig. 4. Distribution of principal stresses when the cylinder is placed at a depth of 14.5 km. Solid lines denote tensile stresses and broken lines compression.

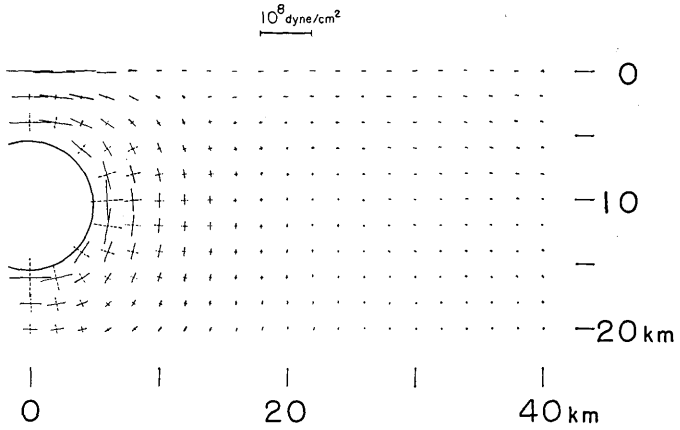

Fig. 5. Distribution of principal stresses when the cylinder is placed at a depth of 10.5 km. Solid lines denote tensile stresses and broken lines compression.

become small when the cylinder is situated at a depth much larger than the radius of the cylinder. They have been estimated to be of the order of $(a/f)^3$ in the case of a sphere being embedded in the earth.[12] In the cylindrical case, they can properly be supposed to be of the order of $(a/f)^2$. Numerically calculated values of the normal stress on the cylindrical surface were confirmed to vary within 30% of the prescribed value.

3. Magnetic changes

In this section, changes in magnetization due to stress effect are calculated numerically, based on the stress distribution obtained in the previous section. It is assumed here that the isotherm of the Curie temperature lies at a depth of 20 km and that no contribution to the field change at the surface is made from beneath the 20 km depth.

We shall denote the major component of the principal stress by $\delta\tau_M$ and the minor one by $\delta\tau_m$. Let J_M and δJ_M be the magnetization in the direction of the major axis of the principal stress and the change in the magnetization due to stress effect in the same direction. J_m and δJ_m are the corresponding quantities along the minor axis. Then we have

$$\delta J_M = (k_1\delta\tau_M + k_2\delta\tau_m)J_M \ ,$$
$$\delta J_m = (k_2\delta\tau_M + k_1\delta\tau_m)J_m \ ,$$

where k_1 is the constant representing the stress effect on the magneti-

12) *ibid.*, 10).

zation in the direction of the applied stress while k_2 represents the stress effect orthogonal to the applied stress.

x and z components of the magnetization vector $(\delta J_x, \delta J_z)$ are obtained by the simple transformation,

$$\delta J_x = \delta J_M \cos\varphi + \delta J_m \sin\varphi ,$$
$$\delta J_z = \delta J_M \sin\varphi - \delta J_m \cos\varphi ,$$

In the present two dimensional case, magnetic potentials due to magnetization changes δJ_x and δJ_z are written as follows,

$$\left.\begin{aligned} W_1 &= \iint \frac{2\delta J_x(x', z')\cdot(x-x')}{(x-x')^2+(z-z')^2}\,dx'dz' , \\ W_2 &= \iint \frac{2\delta J_z(x', z')\cdot(z-z')}{(x-x')^2+(z-z')^2}\,dx'dz' , \end{aligned}\right\} \qquad (7)$$

where (x, z) denotes the coordinate of the observation point. Then the magnetic change $(\Delta H_x, \Delta H_z)$ observed at a point (x, z) become

$$\left.\begin{aligned} \Delta H_x &= \iint [\delta H_x^1 + \delta H_x^2]dx'dz' , \\ \Delta H_z &= \iint [\delta H_z^1 + \delta H_z^2]dx'dz' , \end{aligned}\right\} \qquad (8)$$

where

$$\left.\begin{aligned} \delta H_x^1 &= 2\delta J_x(x', z')\frac{(x-x')^2+(z-z')^2}{\{(x-x')^2+(z-z')^2\}^2} , \\ \delta H_x^2 &= 4\delta J_z(x', z')\frac{(x-x')(z-z')}{\{(x-x')^2+(z-z')^2\}^2} , \\ \delta H_z^1 &= 4\delta J_x(x', z')\frac{(x-x')(z-z')}{\{(x-x')^2+(z-z')^2\}^2} , \\ \delta H_z^2 &= -2\delta J_z(x', z')\frac{(x-x')^2-(z-z')^2}{\{(x-x')^2+(z-z')^2\}^2} . \end{aligned}\right\}$$

The integration should be carried out over the region $0 \leqq z' \leqq 20$ km, $-\infty < x' < \infty$, excepting the cylindrical area, where it is assumed here that the stress has no effect on the magnetization change.

Analytical treatment of the integrals (8) seems impossible when the changes in magnetization calculated in the previous section are introduced in the integrand of the equations (8). It is attempted, therefore, to calculate the equations (8) numerically in this paper.

A problem of convergence arises if the equations (8) are integrated numerically. When x' and z' approach to x and z respectively, δH_x^1, for

example, increases infinitely for a finite δJ_x. In order to avoid this difficulty, δH_x^1, δH_x^2, δH_z^1 and δH_z^2 are analytically calculated first within the interval $[x_i-\Delta x, x_i+\Delta x]$, assuming that δJ_x and δJ_z remain constant within the region. Here Δx is half of the unit length of each mesh point for which the variation in magnetization is calculated.

$$\Delta H_x^{1i}=\int_{x_i-\Delta x}^{x_i+\Delta x}\delta H_x^1 dx'=2\delta J_x(x_i, z')\left[\frac{x-x'}{(x-x')^2+(z-z')^2}\right]_{x_i-\Delta x}^{x_i+\Delta x},$$

$$\Delta H_x^{2i}=\int_{x_i-\Delta x}^{x_i+\Delta x}\delta H_x^1 dx'=2\delta J_z(x_i, z')\left[\frac{z-z'}{(x-x')^2+(z-z')^2}\right]_{x_i-\Delta x}^{x_i+\Delta x},$$

$$\Delta H_z^{1i}=\int_{x_i-\Delta x}^{x_i+\Delta x}\delta H_z^1 dx=2\delta J_x(x_i, z')\left[\frac{z-z'}{(x-x')^2+(z-z')^2}\right]_{x_i-\Delta x}^{x_i+\Delta x},$$

$$\Delta H_z^{2i}=\int_{x_i-\Delta x}^{x_i+\Delta x}\delta H_z^2 dx'=-2\delta J_z(x_i, z')\left[\frac{x-x'}{(x-x')^2+(z-z')^2}\right]_{x_i-\Delta x}^{x_i+\Delta x}.$$

Then summation is taken over i as follows,

$$\Delta H_x=\int\sum_i(\Delta H_x^{1i}+\Delta H_x^{2i})dz',$$

$$\Delta H_z=\int\sum_i(\Delta H_z^{1i}+\Delta H_z^{2i})dz'.$$

There still remains the problem of integration when z' approaches to z. In the following calculation, it is assumed that the observation is always conducted 10 m above the ground surface, i.e. $z=-10^3$cm. Integration for z' is carried out by Simpson's rule, by dividing z' finely for the shallower part, i.e., δJ_x and δJ_z are calculated at the interval of 1 m for $0\leqq z'\leqq 10$ m, 10 m for $10\,\text{m}<z'\leqq 100$m, 100m for $100\text{m}<z'\leqq 1$km and 1km for $1\text{km}<z'\leqq 20$km.

Although there are no satisfactory experiments as yet on the piezomagnetic effect on the remanent magnetization of rocks, k_1 and k_2 are tentatively assumed as 1.0×10^{-10}cm^2/dyne and -0.5×10^{-10}cm^2/dyne respectively, following Stacey[13].

Changes in magnetization and hence changes in the magnetic field caused by stress changes in the previous section are calculated in the case where the earth is composed of a homeogeneous rock magnetized with an intensity of 3×10^{-3}emu/cc.

For the purpose of examining the numerical procedure, the magnetization and the field change are calculated for the case of zero magnetic

13) *ibid.*, 7).

inclination where the geomagnetic field is horizontal. In Fig. 6, changes in magnetization J_x and J_z are shown when the cylinder is situated at a depth of 14.5km and a pressure of 10^8 dynes/cm^2 is applied from inside. Field variations at the ground surface caused by the change in the magnetization are shown in Fig. 7. As a matter of cource, distributions in the field change become symmetrical along the meridian for the north component (ΔX) and the total intensity (ΔF). Differences between the maxima of positive and negative field variation amount to 2.9γ in ΔX, 2.8γ in ΔZ and 2.9γ in ΔF.

When the inclination is 50°, distributions of magnetization and field changes are calculated for the different depths of the cylinder, i.e. 14.5km and 10.5km. Results are shown in Figs. 8 through 11. When the source cylinder of 5km radius is at a depth of 14.5km, the maximum change of 1.7γ in the total field is expected at the surface. The difference in the field variation amounts to 2.5γ in ΔF. When the source is at a depth of 10.5km, the maximum change in the total intensity amounts to 2.7γ and the largest difference between the field variation in ΔF reaches 5.3γ.

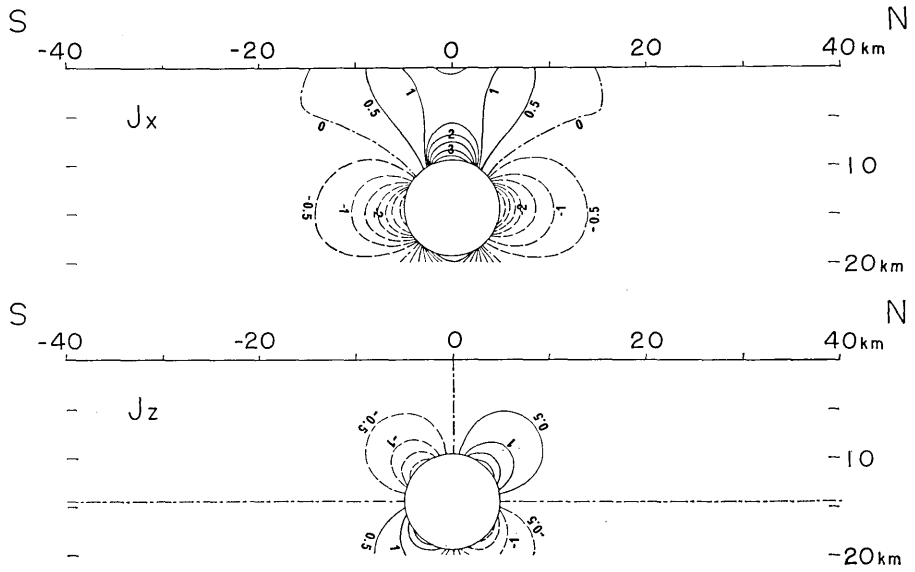

Fig. 6. Changes in magnetization for a homogeneous earth having an intensity of 3×10^{-3}emu/cc, the magnetic inclination being zero. Unit is 10^{-5}emu/cc.

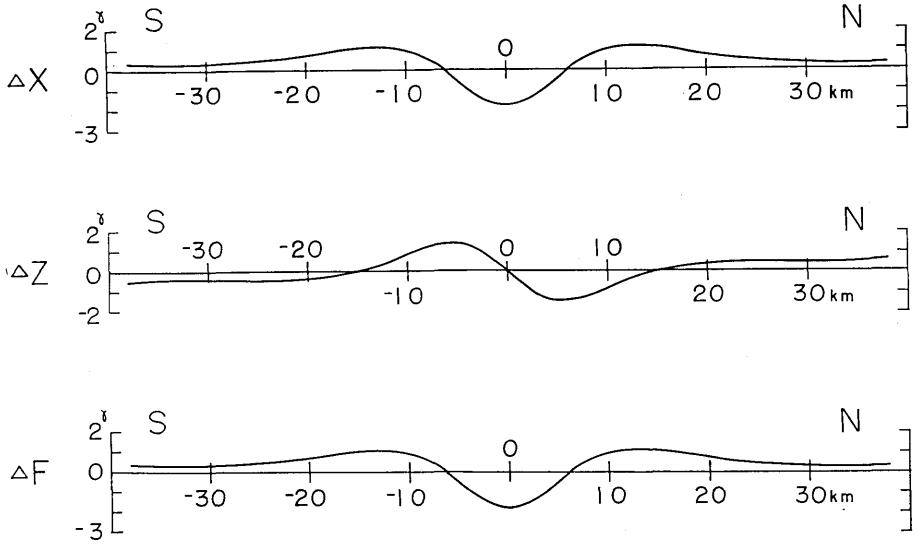

Fig. 7. Changes in the magnetic field along a meridian when the inclination is zero. From the top to the bottom, the change in the north component ΔX, the vertical component ΔZ and the total force intensity ΔF.

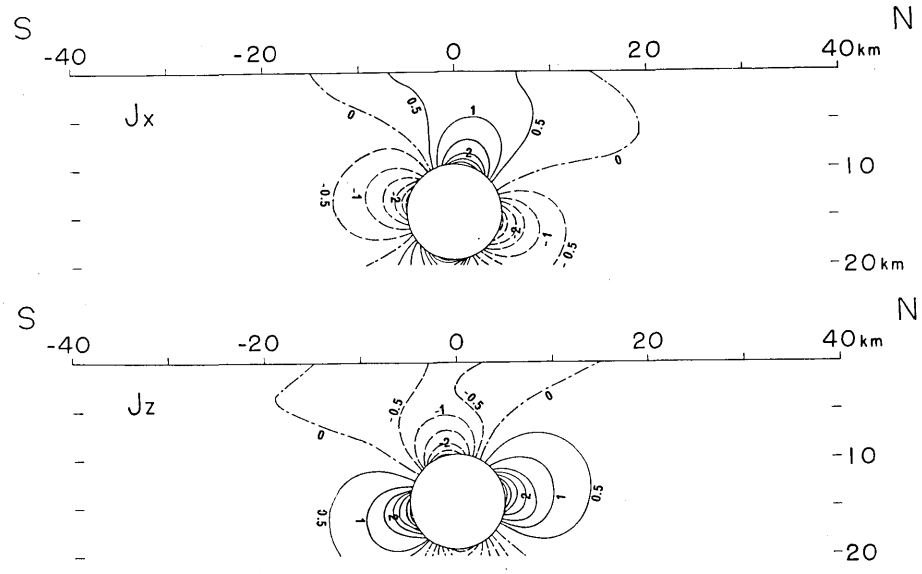

Fig. 8. Changes in magnetization for a homogeneous earth having an intensity of 3×10^{-3}emu/cc, the magnetic inclination being 50°. Unit is 10^{-5}emu/cc.

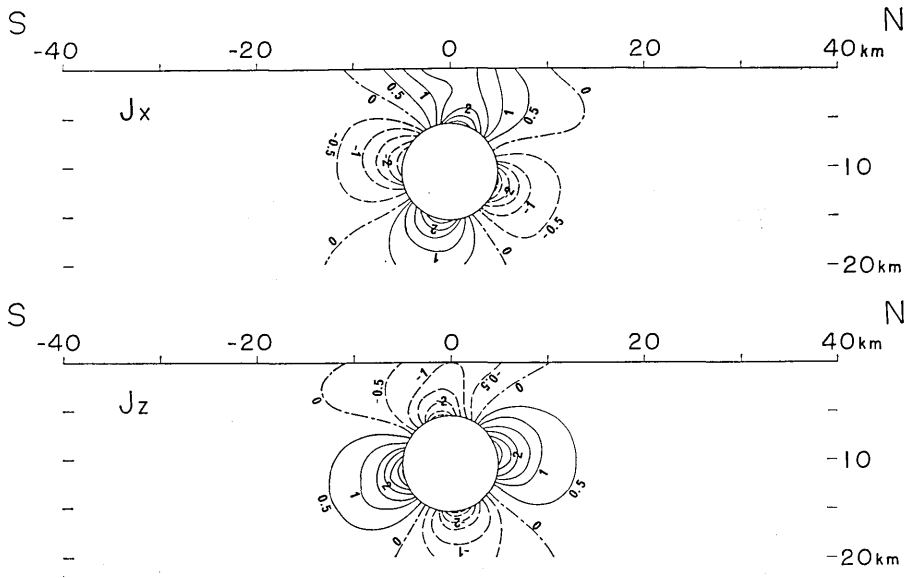

Fig. 9. Changes in magnetization for a homogeneous earth having an intensity of 3×10^{-3}emu/cc, the magnetic inclination being 50°. Unit is 10^{-5}emu/cc.

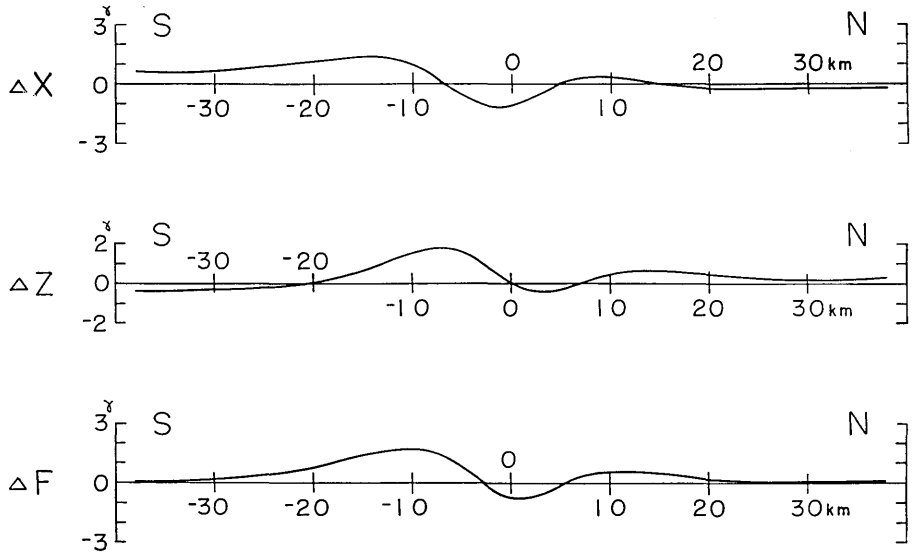

Fig. 10. Changes in the magnetic field along a meridian when the inclination is 50°. From the top to the bottom, the change in the north component ΔX, the vertical component ΔZ and the total force intensity ΔF.

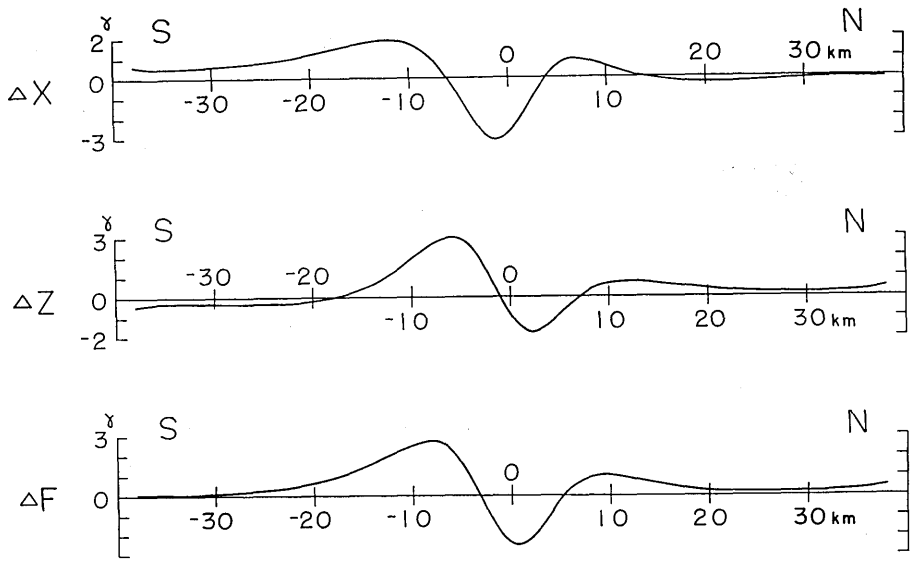

Fig. 11. Changes in the magnetic field along a meridian when the inclination is 50°. From the top to the bottom, the change in the north component ΔX, the vertical component ΔZ and the total force intensity ΔF.

4. Discussion

In the present calculation the earth is assumed homogeneous with a magnetization of 3×10^{-3}emu/cc. The earth is, however, composed of large masses of sedimentary rocks, with much weaker intensity, as well as igneous rocks. When the existence of sedimentary rocks is taken into account, the field variation becomes much less than that obtained here. Actually the complex distribution of the igneous rocks and the sedimentary ones makes the field change much more complicated. In this case, the field gradient may be distributed irregularly and become much larger than the present one, though the field variation itself is lessened.

In this study, it is also assumed that the magnetization inside the cylinder cannot be subject to any change. This may be the case where the material within the cylinder has already met destruction and no stress can accumulate there any longer, or the case where the cylinder is filled with liquid such as a magma reservoir.

The present model gives the maximum strain of 3.4×10^{-5} at the surface, whereas strain changes of 10^{-4} were often observed at the time

of earthquakes.[14),15)] Although it is difficult to infer the real distributions of stress and strain within the earth, those calculated in this paper seem to give a rather moderate order of magnitude for estimating the change in the geomagnetic field which may be associated with an earthquake.

At the time of the Matsushiro earthquakes, gradual changes in the magnetic field have been reported at two stations approximately 6km apart from each other at the time of the most seismically active periods.[16)] At a northern station the total intensity decreased about 5γ during 2 months, while at a southern station the total intensity increased by approximately the same amount. Although the earth is not composed of a single homogeneous rock as in the model studied here, nor is the earthquake mechanism so simple as assumed in this paper, it is still interesting to point out that the total force intensity decreases in the north and increases in the south of the cylinder (or epicentral area) and that the order of magnitude of the change is, in the case of the cylinder located at a depth of 10.5km, not very different from the observed variation in Matsushiro.

Acknowledgments

The writers wish to express their thanks to Prof. T. Rikitake who kindly allowed them to use his unpublished work. Dr. K. Mogi is acknowledged for his helpful discussion on the stress-strain distributions.

---

41. 円筒状力源による半無限弾性体内の応力分布とそれに伴う地磁気変化

地震研究所 行武毅, 立中ひろ子

地下に円筒状の力源があり，その表面に内部から静水圧が加つた場合の，地中の応力分布と，それに伴う地磁気変化とを計算した．地殻が深さ 20 km まで自然残留磁気 3×10^{-3} emu の一様な岩からなり，半径 5 km の円筒が，深さ 14.5 km にあつて，内側から 100 bar の圧力が加つた場合，地表では最大 2γ の全磁力の変化が期待される．深さ 10.5km の円筒に対しては，地表の変化は 3γ に達する．

---

14) C. TSUBOI, *Jap. Jour. Astr. Geophys.*, **10** (1933), 93.

15) K. KASAHARA, A. OKADA, M. SHIBANO, K. SASAKI and S. MATSUMOTO, *Bull. Earthq. Res. Inst.*, **44** (1966), 1715.

16) T. RIKITAKE, Y. YAMAZAKI, M. SAWADA, Y. SASAI, T. YOSHINO, S. UZAWA and T. SHIMOMURA, *Bull. Earthq. Res. Inst.*, **44** (1966), 1735.